Letter
Vol. 5, No. 5 / May 2018 / Optica 514

optica

Independent high-purity photons created in domain-engineered crystals

FRANCESCO GRAFFITTI,* PETER BARROW, MASSIMILIANO PROIETTI, DMYTRO KUNDYS, AND ALESSANDRO FEDRIZZI

Scottish Universities Physics Alliance (SUPA), Institute of Photonics and Quantum Sciences, School of Engineering and Physical Sciences, Heriot-Watt University, Edinburgh EH14 4AS, UK
**Corresponding author: fraccalo@gmail.com*

Received 22 December 2017; revised 23 March 2018; accepted 4 April 2018 (Doc. ID 318273); published 30 April 2018

Advanced photonic quantum technology relies on multi-photon interference, which requires bright sources of high-purity photons. Single-photon sources based on nonlinear parametric processes typically require lossy spectral filtering for enhancing the spectral purity of the heralded photons. Here, we implement a novel domain-engineering technique for tailoring the nonlinearity of a parametric down-conversion crystal in order to generate indistinguishable and spectrally pure photons without filtering. We create pairs of independently heralded telecom-wavelength photons with high heralding efficiency (up to 65%) and brightness (4 kHz/mW), and we demonstrate a high lower bound for the indistinguishability ($98.7 \pm 0.2\%$) and spectral purity ($90.7 \pm 0.3\%$) via two-photon interference experiments.

OCIS codes: (270.0270) Quantum optics; (270.5585) Quantum information and processing; (270.6570) Squeezed states.

https://doi.org/10.1364/OPTICA.5.000514

Quantum photonics with single photons is a leading platform suitable for all aspects of quantum information processing—quantum computing and simulation, communication, and metrology. Multi-photon schemes such as recent proposals for loss-robust photonic cluster-state percolation [1] rely on a high number of successive two-photon interference events: any reduction in interference visibility leads to a drastic resource-cost increase in the required number of photon sources, detectors, and circuit complexity [2,3]. Since perfect interference can be achieved only with pure and indistinguishable photons [4], the development of high-quality single-photon sources is essential. A wide range of single-photon emitters is under development, typically classified into single-quantum emitters such as quantum dots [5] and parametric optical processes. The quality of photons and brightness of quantum dot sources is ever increasing; however, in many cases, parametric downconversion (PDC) in nonlinear crystals still provides a simpler, higher-quality solution especially at telecommunication wavelengths.

A central requirement for producing high-purity heralded photons via PDC is to remove the spectral correlations in the photon pairs that arise due to energy and momentum conservation: typically, narrow filters are employed to increase purity at the expense of brightness and heralding efficiency. This tradeoff can be overcome with three tricks known under the umbrella of "group-velocity matching" (GVM) [6–8]: (i) the group velocities of the PDC photons and pump laser need to be matched; (ii) the respective spectral bandwidths need to match; and (iii) the longitudinal nonlinearity profile of the PDC crystal needs to be Gaussian to remove residual correlations arising from the *sinc*-shaped phase-matching function (PMF) associated with standard crystals [9] (see Fig. 1). Techniques for tailoring crystal nonlinearities have only recently been adapted from the classical regime to the creation of spectrally pure photons [9–13]. Proof-of-principle demonstrations have verified that domain-engineered crystals can indeed create photons with approximated Gaussian spectra [9,11,14]. However, a reliable benchmark of the spectral purity achieved for single photons independently created in apodized crystals under GVM conditions has so far not been set.

Here, we implement a recently developed nonlinear crystal domain-engineering algorithm [10] in a group-velocity-matched regime at telecommunication wavelengths and demonstrate two-photon interference between heralded photons created in independent PDC processes. We simultaneously achieve high brightness, heralding efficiencies, signal-idler indistinguishability, and single-photon spectral purity without the use of lossy spectral filters. Importantly, our scheme creates symmetric heralding conditions, meaning that our photon sources are suitable not only for heralding single photons but also scalable to larger multi-photon protocols.

We first consider the first-order PDC bi-photon state:

$$|\psi_{\text{pair}}\rangle_{s,i} = \iint \mathrm{d}\omega_s \mathrm{d}\omega_i f(\omega_s, \omega_i) \hat{a}_s^\dagger(\omega_s) \hat{a}_i^\dagger(\omega_i) |0\rangle_{s,i}, \quad (1)$$

where s (i) denotes the signal (idler) photon. The joint spectral amplitude (JSA) $f(\omega_s, \omega_i)$ depends on the spectral properties of the pump and the PMF [6], which itself depends on the nonlinear properties of the crystal. Whenever the detection of one photon of a pair heralds the presence of another, the spectral purity of the signal photon decreases as the signal-idler spectral correlations increase [7]. The JSA therefore has to be separable in order to generate pure photons.

To achieve that, we designed an apodized potassium titanyl phosphate (aKTP) crystal using the domain-engineering annealing algorithm introduced in Ref. [10], and we compare its performance with a periodically poled KTP (ppKTP). Starting from a seed poling period of 46.22 μm, our algorithm chooses each ferroelectric domain's orientation and width in order to shape the overall crystal PMF as a Gaussian function [Fig. 1(b)]. The crystals are phase matched for type-II PDC and produce two orthogonally polarized photons with central wavelength of 1550 nm and 1.5 nm bandwidth, estimated from the marginal spectral distributions of the $|\mathrm{JSA}|^2$. Perfect GVM in KTP crystals is achieved when the pump has a Gaussian spectral envelope centered at 791 nm [7]: in these conditions, single-photon spectral purity from a standard ppKTP would be ~81.4%, compared to ~97.9% purity for our apodized crystal. Our experimental implementation slightly deviates from the ideal case though. First, mode-locked laser pulses have a sech^2-shaped intensity envelope. Second, the crystal length of 29 mm for the aKTP and 22 mm for the ppKTP is chosen to match the corresponding PMF full-width half-maximum (FWHM) of both crystals to a transform-limited sech^2 pulse centered at 775 nm and of 1.4 ps duration (defined as the FWHM of the pulse intensity envelope). However, our laser has a 1.7 ps pulse length, and the resulting JSA is slightly elliptical (Fig. 1). Under these conditions, we estimate single-photon purities of 80.1% and 95.3% for the standard and engineered crystals, respectively. These values define an upper bound for the experimentally achievable two-photon interference visibilities for independently heralded photons.

Our experimental setup is shown in Fig. 2. Our counting logic records the coincidences (cc) within a 1 ns time window between single photons (s_i) detected by the superconducting nanowire single-photon detectors (SNSPDs): we measure a

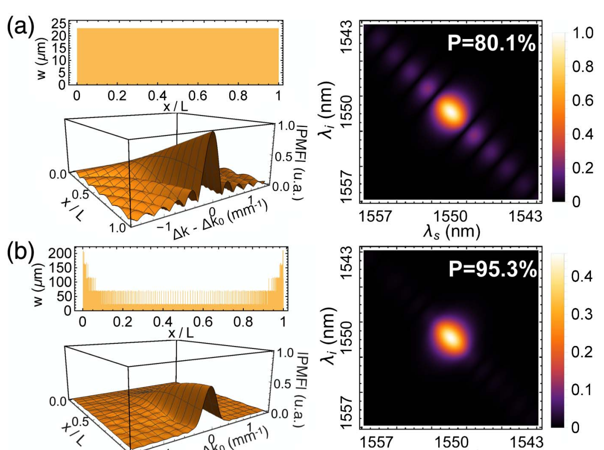

Fig. 1. Crystal domain-width (w) pattern (top-left), PMF along the crystal (bottom-left), and simulated JSA (right) for the ppKTP (a) and aKTP (b). The Δk depends on the signal-idler frequencies according to the Sellmeier equations used in Ref. [10]. The heralded-photon spectral purity is computed via a numerical Schmidt decomposition on the discretized JSA [15].

source brightness of (11.25 ± 0.08) kHz/mW and (4.02 ± 0.04) kHz/mW of detected pairs for the ppKTP and the aKTP, respectively, and a four-photon rate for two independent sources of $(1.52 \pm 0.02)\ \mathrm{Hz/mW}^2$ and $(0.19 \pm 0.01)\ \mathrm{Hz/mW}^2$. We estimate a symmetric heralding efficiency $\eta = \mathrm{cc}/(\sqrt{s_1 s_2})$ of 53% in the configuration used for the experiment, but a value of η up to 65% is achieved with the same crystals under loose focusing conditions [16], at the expense of brightness: this corresponds to a collection efficiency of 88.5% once detector efficiency (80%) and known optical losses of (7.6%) are accounted for.

To estimate spectral photon purity from group-velocity-matched PDC sources, it is common practice to measure the bi-photon joint spectral intensity (JSI). The JSI can be measured with a pair of grating spectrometers, with dispersion spectroscopy [14], or via stimulated emission tomography [17,18]. However, the accuracy and precision of these measurements is often limited due to poor signal-to-noise ratios and a tradeoff between spectral range and resolution. Focusing on the central JSI peak in return for increased spectral resolution truncates correlations in the PMF side lobes, which are required for reliable purity estimation. To illustrate this for the standard ppKTP in Fig. 1, restricting the JSA to just the central peak increases the apparent purity calculated via the Schmidt decomposition from 80.1% to 93.2%. Furthermore, the JSI does not capture phase information. Performing the Schmidt decomposition on the square root of the JSI instead of the JSA for the same crystal yields a purity of 82.7% instead of 80.1%.

A more reliable benchmark for single-photon purity and indistinguishability is therefore the direct observation via two-photon interference. Interference between photons generated in the same PDC process gives an estimate of signal-idler indistinguishability [19]. More importantly, the two-photon interference visibility $(N_{\max} - N_{\min})/N_{\max}$ between heralded photons, where $N_{\max}$ ($N_{\min}$) is the maximum (minimum) number of coincident photon detections, corresponds to a direct measurement of single-photon purity [4].

This purity includes both the spectral as well as the photon-number degree of freedom. The photon number state of heralded PDC photons is typically mixed due to multi-photon emissions. While this is an intrinsic limitation of PDC, it can be mitigated to an arbitrary degree by multiplexing [20–23] and single-photon post-selection enabled by number-resolved detectors [24]. One can, however, obtain a lower bound on just the *spectral* purity by measuring interference versus pump power, as we outline below.

Omitting the spectral wavefunction, the PDC state in the Fock space is

$$|\psi_{\mathrm{PDC}}\rangle = \sqrt{1 - |\lambda|^2} \sum_{n=0}^{\infty} \lambda^n |n\rangle_s |n\rangle_i, \tag{2}$$

where n is the photon number. The parameter λ relates to source brightness [20] and can be expressed as a function of the pump power P and of the constant τ, determined by the efficiency of the nonlinear process, the detection efficiency and optical loss in the setup: $\lambda = \sqrt{P\tau}$. Since perfect two-photon interference occurs when two and only two identical photons enter the 50-50 beam splitter (BS), all terms proportional to $|n > 1\rangle_s |n > 1\rangle_i$ in Eq. (2) compromise the interference visibility. In the limit of low pump power and negligible detector noise, the two-photon visibility decreases linearly with increasing P (see Supplement 1 for details); therefore, we can extrapolate a visibility V_0 from measurements over a range of P (i.e., for a range of $\lambda \to 0$). V_0 provides a lower bound for the indistinguishability (in the case of signal-idler interference) and single-photon spectral purity (for two interfering heralded photons).

We first estimate the signal-idler indistinguishability by interfering photons produced in the same PDC process [see Fig. 2(c)] at different P. Figure 3(a) shows two-photon interference patterns for the ppKTP and the aKTP at low pump power without spectral filtering. Being in symmetric-GVM condition, the two-photon interference pattern can be approximated by the convolution of the PMF with itself [25]: as expected, it is almost triangular for the standard crystal [26], and Gaussian for the custom design. We find an indistinguishability V_0 of $(99.7 \pm 0.1)\%$ for the ppKTP and $(98.7 \pm 0.1)\%$ for the aKTP (see Supplement 1 for details). This signal-idler indistinguishability is, to our knowledge, the highest reported so far with an apodized crystal.

Ideally, measuring the spectral purity of a PDC photon requires the interference of two copies of the same photon [4]. The quantum state of a photon cannot be cloned, and the most faithful purity estimate is therefore obtained from interfering two photons emitted in short succession from the same crystal. In our setup, Fig. 2(b), we send the first heralded photon into a fiber delay line and a second into a shorter fiber before superposing them on a fiber beam splitter. This succeeds with probability 1/4, and we chose a delay of five pump pulses to exceed the ~60 ns SNSPD reset time. The two interfering photons are heralded by their respective twins, and four-photon coincidences are recorded. We extrapolate a V_0 of $(79.6 \pm 0.1)\%$ for the standard ppKTP, which matches theory expectations (see Fig. 1) and a V_0 of $(90.7 \pm 0.3)\%$ with the apodized crystals [see Fig. 3(b)]. We then interfere and detect photons produced by two different aKTP crystals [Fig. 2(d)] to show that our technique is feasible for multi-photon experiments. We also detect the idler photons and collect the overall number of fourfold coincidences from the four SNSPDs. In this configuration, we find a V_0 of $(89.8 \pm 0.2)\%$ [Fig. 3(b)].

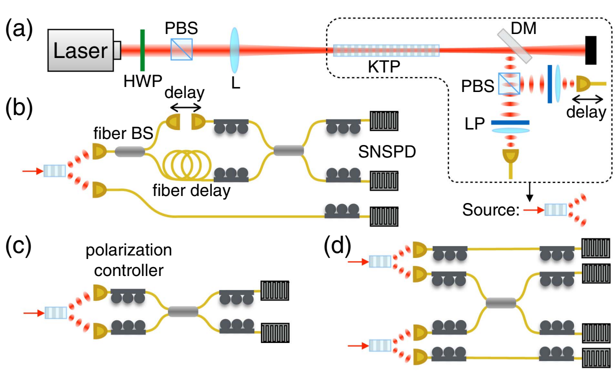

Fig. 2. Schematic of the experimental setup. (a) An 80 MHz repetition rate Ti-Sapphire laser is focused into the crystal where it generates 1550 nm PDC photons. These are split at a PBS and collected in single-mode fibers to be used in setups 2 (b)–(d). Laser light is removed with a dichroic mirror (DM) and long-pass filters (LP) The photons are detected by SNSPDs. We observe two-photon interference for: (b) photons created in the same setup at different times; (c) photons created in a single PDC process. (d) Photons created in two separate crystals.

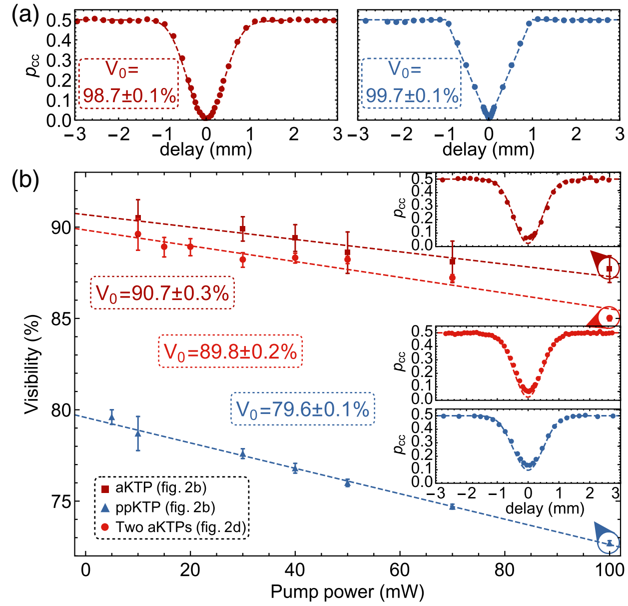

Fig. 3. (a) Two-photon interference as a function of temporal delay between photons generated by the same PDC process in the ppKTP (right) and the apodized crystal (left). Data are normalized against a coincidence probability of 1/2 outside the interference region. (b) Interference visibilities at different pump powers for the two experimental schemes in Figs. 2(b) and 2(d). The dashed lines are the simulated interference pattern obtained from the JSA in Fig. 1, while the visibilities are obtained from Gaussian fits. Statistical uncertainties on the visibilities of each interference experiment are estimated from 5000 samples of a Monte Carlo routine based on the Poissonian counting statistics of the experiment [27].

We can increase the quality of the photons produced with the aKTP, by applying "gentle" spectral filtering. We use a bandpass filter with a spectral transmission of the form $\exp[-\frac{(\omega-\omega_0)^4}{2\sigma^4}]$, centered at 1550 nm and a FWHM of 7.4 nm, which is roughly five times larger than the PDC bandwidth. This filter decreases heralding efficiency by no more than 1%—and in this configuration, we achieve a heralded-photon purity of $(92.7 \pm 0.2)\%$ and a signal-idler indistinguishability of $(99.7 \pm 0.1)\%$ (see Supplement 1 for details). This value is close to the maximum visibility we can achieve (99.8%) due to imperfect optics.

The V_0 corresponding to the apodized crystals shown in Fig. 3(a) are significantly higher than for the standard KTPs: however, they are still somewhat short of expectations (Fig. 1). Our fiber BS has a reflectivity (transmissivity) of 49.2% (50.8%), and the polarizing BS (PBS) leaks 0.5% of opposite polarized photons—a visibility decrease of ~0.2% for independent photon sources. Some degradation may be due to random duty-cycle errors occurring during crystal fabrication. To assess this error, we numerically vary each domain's width according to a Gaussian distribution with 1 μm FWHM and for each instance compute the JSA and corresponding photon purity. We find a decrease of the mean single-photon purity of about 0.3%, with a final value of $P = (95.0 \pm 0.2)\%$. Finally, the imperfect indistinguishability of the signal-idler photons, and its increase under gentle filtering suggests the presence of undesirable PDC generation far from the central JSA peak, which is not present in the standard ppKTP.

In Fig. 4, we assess the impact of spectral filtering on the heralding efficiency and the single-photon purity of our photon

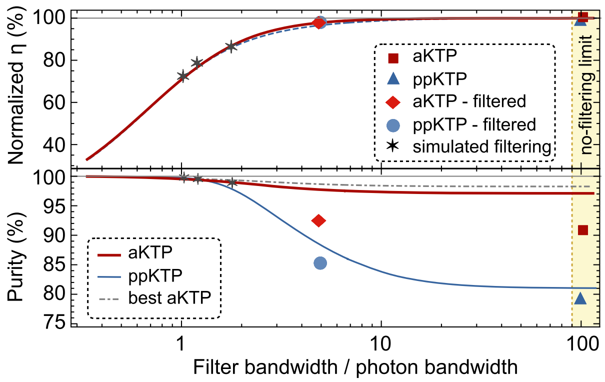

Fig. 4. Normalized heralding and purities for the ppKTP (blue) and the aKTP (red) under spectral filtering. The light-blue and light-red data points correspond to the ppKTP and aKTP with gentle filtering, while the dark gray stars represent three commercial bandpass filters (left to right: Iridian Spectral Technologies Ltd., Alluxa, Omega Optical Inc.) applied to the ppKTP. The dot-dashed gray line shows the simulated purity for a crystal tailored with optimal domain engineering [10].

sources. The normalized heralding represents the maximum heralding achievable, factoring out known losses, detection, and collection efficiency, while the x axis is the ratio between the filter and single-photon bandwidth. The data correspond to our setup, and the simulated heralding and purities hold in general for ppKTP/aKTP crystals of arbitrary length when group-velocity matched with a sech^2 pulse. We see a drastic tradeoff between spectral purity and heralding efficiency for photons created in standard ppKTP: A 99% purity can be achieved when a filter with twice the PDC bandwidth is applied to both photons. However, even ideal filters with 100% peak transmission would decrease the heralding efficiency to 80%, and the source brightness to 60%, which in a modest six-photon experiment would amount to a drop in observed rates to just 22%. In contrast, our apodized crystal sources operate in, or at least very close to, the "no-filtering" limit, overcoming this tradeoff. By fixing all known minor problems—fine tuning the domain-engineering algorithm, shaping a Gaussian pump pulse at 791 nm, and suppressing PDC noise—we are confident we can push the lower bound on spectral purity to at least 95% in the near future.

Funding. Engineering and Physical Sciences Research Council (EPSRC) (EP/L015110/1, EP/N002962/1).

Acknowledgment. The authors thank A. M. Brańczyk for useful discussions and A. Pickston and M. Ringbauer for experimental assistance.

See Supplement 1 for supporting content.

REFERENCES

1. M. Gimeno-Segovia, P. Shadbolt, D. E. Browne, and T. Rudolph, Phys. Rev. Lett. **115**, 020502 (2015).
2. Y. Li, S. D. Barrett, T. M. Stace, and S. C. Benjamin, Phys. Rev. Lett. **105**, 250502 (2010).
3. E. Meyer-Scott, N. Montaut, J. Tiedau, L. Sansoni, H. Herrmann, T. J. Bartley, and C. Silberhorn, Phys. Rev. A **95**, 061803 (2017).
4. A. M. Brańczyk, arXiv preprint arXiv:1711.00080 (2017).
5. P. Senellart, G. Solomon, and A. White, Nat. Nanotechnol. **12**, 1026 (2017).
6. W. P. Grice, A. B. U'Ren, and I. A. Walmsley, Phys. Rev. A **64**, 063815 (2001).
7. A. B. U'Ren, C. Silberhorn, R. Erdmann, K. Banaszek, W. P. Grice, I. A. Walmsley, and M. G. Raymer, arXiv preprint quant-ph/0611019 (2006).
8. P. J. Mosley, J. S. Lundeen, B. J. Smith, and I. A. Walmsley, New J. Phys. **10**, 093011 (2008).
9. A. M. Brańczyk, A. Fedrizzi, T. M. Stace, T. C. Ralph, and A. G. White, Opt. Express **19**, 55 (2011).
10. F. Graffitti, D. Kundys, D. T. Reid, A. M. Brańczyk, and A. Fedrizzi, Quantum Sci. Technol. **2**, 035001 (2017).
11. P. B. Dixon, J. H. Shapiro, and F. N. C. Wong, Opt. Express **21**, 5879 (2013).
12. A. Dosseva, Ł. Cincio, and A. M. Brańczyk, Phys. Rev. A **93**, 013801 (2016).
13. J.-L. Tambasco, A. Boes, L. G. Helt, M. J. Steel, and A. Mitchell, Opt. Express **24**, 19616 (2016).
14. C. Chen, C. Bo, M. Y. Niu, F. Xu, Z. Zhang, J. H. Shapiro, and F. N. C. Wong, Opt. Express **25**, 7300 (2017).
15. F. Laudenbach, H. Hübel, M. Hentschel, P. Walther, and A. Poppe, Opt. Express **24**, 2712 (2016).
16. L. K. Shalm, E. Meyer-Scott, B. G. Christensen, P. Bierhorst, M. A. Wayne, M. J. Stevens, T. Gerrits, S. Glancy, D. R. Hamel, M. S. Allman, K. J. Coakley, S. D. Dyer, C. Hodge, A. E. Lita, V. B. Verma, C. Lambrocco, E. Tortorici, A. L. Migdall, Y. Zhang, D. R. Kumor, W. H. Farr, F. Marsili, M. D. Shaw, J. A. Stern, C. Abellán, W. Amaya, V. Pruneri, T. Jennewein, M. W. Mitchell, P. G. Kwiat, J. C. Bienfang, R. P. Mirin, E. Knill, and S. W. Nam, Phys. Rev. Lett. **115**, 250402 (2015).
17. M. Liscidini and J. E. Sipe, Phys. Rev. Lett. **111**, 193602 (2013).
18. A. Eckstein, G. Boucher, A. Lemaître, P. Filloux, I. Favero, G. Leo, J. E. Sipe, M. Liscidini, and S. Ducci, Laser Photon. Rev. **8**, L76 (2014).
19. V. Giovannetti, L. Maccone, J. H. Shapiro, and F. N. C. Wong, Phys. Rev. A **66**, 043813 (2002).
20. M. A. Broome, M. P. Almeida, A. Fedrizzi, and A. G. White, Opt. Express **19**, 22698 (2011).
21. M. J. Collins, C. Xiong, I. H. Rey, T. D. Vo, J. He, S. Shahnia, C. Reardon, T. F. Krauss, M. J. Steel, A. S. Clark, and B. J. Eggleton, Nat. Commun. **4**, 2582 (2013).
22. C. Xiong, X. Zhang, Z. Liu, M. J. Collins, A. Mahendra, L. G. Helt, M. J. Steel, D.-Y. Choi, C. J. Chae, P. H. W. Leong, and B. J. Eggleton, Nat. Commun. **7**, 10853 (2016).
23. F. Kaneda, F. Xu, J. Chapman, and P. G. Kwiat, Optica **4**, 1034 (2017).
24. V. D'Auria, O. Morin, C. Fabre, and J. Laurat, Eur. Phys. J. D **66**, 249 (2012).
25. M. Barbieri, E. Roccia, L. Mancino, M. Sbroscia, I. Gianani, and F. Sciarrino, Sci. Rep. **7**, 7247 (2017).
26. A. Fedrizzi, T. Herbst, M. Aspelmeyer, M. Barbieri, T. Jennewein, and A. Zeilinger, New J. Phys. **11**, 103052 (2009).
27. N. K. Langford, "Encoding, manipulating and measuring quantum information in optics," Ph.D. thesis (University of Queensland, 2007).